International Immunopharmacology 69 (2019) 126–135

Contents lists available at ScienceDirect

International Immunopharmacology

journal homepage: www.elsevier.com/locate/intimp

Mmu-miR-92a-2-5p targets TLR2 to relieve *Schistosoma japonicum*-induced liver fibrosis

Yumin Zhao[a], Zhisheng Dang[b], Shigui Chong[c,*]

[a] Department of Parasitology, Guilin Medical University, Guilin 541004, Guangxi, China
[b] Key Laboratory on Biology of Parasite and Vector, Ministry of Health, Parasitic Disease Control Center of China Center for Disease Control and Prevention, Shanghai 200025, China
[c] School of Nursing, Guilin Medical University, Guilin 541001, Guangxi, China

ARTICLE INFO

Keywords:
mmu-miR-92a-2-5p
Schistosoma japonicum
Liver fibrosis
TLR2

ABSTRACT

According to conservative estimates, > 230 million people are infected with schistosomiasis,which becomes one of the most common parasitic diseases. This study focuses on investigating in vivo and in vitro effects of mmu-miR-92a-2-5p in *Schistosoma japonicum*-induced liver fibrosis by targeting *TLR2*. Through bioinformatic analysis, the overexpression of *TLR2* and the down-regulation of mmu-miR-92a-2-5p were revealed in the progression of *S. japonicum*-induced liver fibrosis. BALB/C mice were taken advantage to construct normal control and schistosomiasis liver fibrosis (SLF) model. The mice in model groups were transfected recombinant lentivirus (Lenti-mmu-miR-92a-2-5p or Lenti-NC) to alter the expression of mmu-miR-92a-2-5p in vivo. HE and Masson staining were employed to observe the pathological changes and collagenous fibrosis. QRT-PCR showed that mmu-miR-92a-2-5p was decreased while *TLR2* was elevated in the infected groups. However, lenti-mmu-miR-92a-2-5p group could inhibit liver fibrosis. Then the effect of mmu-miR-92a-2-5p on *S. japonicum*-induced liver fibrosis including cell apoptosis rates, proliferation and proteins related to liver fibrosis was examined in NIH-3T3 mouse embryonic fibroblasts. Moreover, the association between mmu-miR-92a-2-5p and *TLR2* was detected by dual-luciferase reporter gene assay and the expression of cytokines IL-4, IFN-γ and TNF-α in SLF model was detected by ELISA. Further, the knockout of *TLR2* in C57BL/6J mice was used to confirm the association between mmu-miR-92a-2-5p and *TLR2*. Thus, these findings demonstrated that mmu-miR-92a-2-5p inhibited *S. japonicum*-induced liver fibrosis by targeting *TLR2* in vitro and in vivo.

1. Introduction

According to conservative estimates, > 230 million people are infected with schistosomiasis resulting in becoming one of the most common parasitic diseases [1,2]. Furthermore, *Schistosoma japonicum* is the only schistosome which could cause infection in China [3]. Schistosoma cercariae could enter the body through the skin dwelling in the tributaries of the portal vasculature, developing into adult worms and then lay eggs [1]. While some potent governmental measures have been taken, for some lakes and marshland regions, the *S. japonicum* is yet severe, which might cause heavy social burdens [4]. Besides, *S. japonicum* infections usually inflict chronic damage and liver fibrosis, even developing into portal hypertension or liver cirrhosis if left untreated [5]. However, the investigation on *S. japonicum* induced liver fibrogenesis is poor, which deserves deeper study.

Toll-like receptors (TLRs), including TLR2, are members of the pattern recognition receptor family, which play a crucial role in non-specific immune system by recognizing some biological macromolecules, such as nucleic acids, carbohydrates, or proteins [6]. The most widely studied members of TLRs are TLR2 and TLR4 in liver diseases, which could sense endogenous ligands triggering a dangerous signal and further induce an inflammatory response, for example, in the axis of hepatic inflammation-fibrosis-carcinoma [7] and hepatocarcinoma [8]. Besides, in the previous study, TLR2 was proven to be involved in hepatic fibrogenesis by regulating MAPK and NF-κB signaling pathways and then influencing the progress of hepatic fibrogenesis [9]. Moreover, the effects of TLR2 had been uncovered in the mice with *S. japonicum* infection, indicating TLR2 knock out promoted T cell response [10]. But, the correlation between TLR2 and liver fibrosis induced by *S. japonicum* infection remains elusive, which might give us a more complete understanding of liver fibrosis.

In according to previous reports, microRNAs (miRNAs), about 22 nt

* Corresponding author at: School of Nursing, Guilin Medical University, No. 20 Lequn Road, Guilin 541001, Guangxi, China.
E-mail address: cjiangshiyang@163.com (S. Chong).

https://doi.org/10.1016/j.intimp.2019.01.007
Received 21 August 2018; Received in revised form 29 December 2018; Accepted 5 January 2019
Available online 29 January 2019
1567-5769/

in size, could be involve in the progress of many diseases through regulating mRNAs targeting their 3'UTR region [11,12]. The crucial role of miRNAs in regulating the proliferation and differentiation of hepatic stellate cells, which, after being activated by liver injury, would differentiate into myofibroblast-like cells [13] to involve in the pathophysiology progress of liver fibrosis had been focused on [14,15]. For example, some miRNAs, miRNA-338-3p [16], miRNA-29 [17] and miRNA-21 [18], which contributed to the activation and proliferation of hepatic stellate cells, had been identified. Moreover, Ye et al. demonstrated that silencing miRNA-145 might target adducin 3 to contribute to liver fibrosis [19]. The deregulation of miRNA-92a-2-5p, a member of the miR-17-92 cluster, was proved to influence a lot of diseases pathophysiology, such as lung cancer [20], but its role in liver fibrosis was not given enough attention. We aimed to investigate the regulatory relation between *TLR2* and miRNA-92a-2-5p and pathological process in liver fibrosis induced by *S. japonicum* infection to get comprehensive understanding of liver fibrosis.

In our study, some deregulating genes and related signal pathways had been identified via bioinformatics analysis for further study. Moreover, dual-luciferase reporter gene assay was employed to detect the relationship between mmu-miR-92a-2-5p and *TLR2*. Besides, animal models with Schistosomiasis liver fibrosis by infection with *S. japonicum* were constructed to evaluate the function of mmu-miR-92a-2-5p via lentivirus mediated transfection and its regulatory effect to *TLR2* on Schistosomiasis liver fibrosis in vivo and in vitro.

2. Materials and methods

2.1. Bioinformatics analysis

Microarray data GSE14367 and GSE63135 used for validation were obtained from Gene Expression Omnibus (GEO) database (http://www.ncbi.nlm.nih.gov/geo/). This dataset of GSE14367 included twenty tissue specimens, including 4, 6 and 7 weeks post infection with *S. japonicum*, uninfected and infected with *S. japonicum* eggs. The dataset of GSE63135 included two groups, control and *S. japonicum* infected. Differentially expressed genes as well as deregulated pathways were uncovered through R language and KEGG database. The threshold used to screen upregulated and downregulated mRNA was $P < 0.05$ and $\log_2$ (FC) > 1 or $\log_2$ (FC) < -1, respectively.

2.2. Constructing animal models

TLR2$^{-/-}$ mice on a C57BL/6J background were purchased from purchased from Model Animal Research Center of Nanjing University (Nanjing, China). Female BALB/c mice of 6–8 weeks old were purchased from Silaikejingda animal company of Changsha (Hunan, China). *S. japonicum* cercariae were obtained from Yueyang Institute of *S. japonicum* Diseases (Yueyang, china), which were released from intermediate host *Snail oncomelania* with *S. japonicum* infection. The animals were allowed staying at room temperature 25 °C and given food and water for a week to adapt to the new environment. To construct the models of liver fibrosis induced by *S. japonicum* infection, 15 ± 2 cercariae of *S. japonicum* were employed to percutaneously inject into TLR2$^{-/-}$ mice and BALB/c mice on their abdomens, and pathogen-free mice were severed as the control group. Part of the obtained liver tissues was stored in liquid nitrogen by quick-freezing for total RNA extraction, and the others were restored in 10% paraformaldehyde for pathological observation. All animal experiments were consent with the animal ethics standard of the Second Affiliated Hospital of Guilin Medical University.

2.3. Lentivirus mediated transfer in vivo

The recombinant Lentivirus (Lenti-mmu-miR-92a-2-5p) and the negative control Lentivirus (Lenti-NC) were provided by Genepharama Company (Shanghai, China). For investigation on mmu-miR-92a-2-5p, BALB/c mice were divided into 4 groups, the uninfected group ($n = 5$ in each time point), control group (infected with *S. japonicum* and injected with PBS, $n = 5$), Lenti-mmu-miR-92a-2-5p group (infected with *S. japonicum* and injected with Lenti-mmu-miR-92a-2-5p, n = 5) and Lenti-NC group (infected with *S. japonicum* and injected with Lenti-NC, $n = 5$).

For study the relationship between mmu-miR-92a-2-5p and *TLR2*, C57BL/6J mice were divided into 4 groups, the control group (infected with *S. japonicum*, $n = 5$), the Lenti-mmu-miR-92a-2-5p group (infected with *S.japonicum* and injected with Lenti-mmu-miR-92a-2-5p, n = 5), the *TLR2* knockout group (TLR2 KO control, TLR2$^{-/-}$ mice infected with *S.japonicum*, $n = 5$), the Lenti-mmu-miR-92a-2-5p TLR2 knockout group (Lenti-mmu-miR-92a-2-5p TLR2 KO control, TLR2$^{-/-}$ mice infected with *S.japonicum* and injected with Lenti-mmu-miR-92a-2-5p, n = 5). Mice were injected with phosphate buffered solution (PBS) or recombinant Lentivirus (1◊10^9 TU/mL, 150 mL) via the tail vein after infection *S. japonicum* for 10 days. After infection 0, 2, 4, 6, 8 and 10 weeks, mice were sacrificed to obtain livers and serum samples. Parts of the liver tissues were fixed in a 4% formaldehyde solution and the remaining tissues were stored at −80 °C.

2.4. Hematoxylin-eosin and Masson staining

Fixed liver tissues in 4% formaldehyde were routinely embedded in paraffin and cut into 4-μm-thick sections. H&E and Masson staining were performed separately on tissue sections. In all groups the HE-stained liver sections were examined to calculate the mean number of hepatic granulomas. For the same liver section, five successive fields (10 × 10) were assessed. Masson's trichrome-stained liver sections were used to estimate the hepatic deposition of collagen. Bright-field images were photographed and the hepatic deposition of collagen was estimated quantitatively by the percentage of the area stained with blue color in all fields (10 × 10) with computer image analysis system (Image-Pro Plus software).

2.5. Cell culture and transfection

NIH/3T3 (3T3 *Mus musculus* Swiss) embryonic fibroblasts and 293T were purchased from the China Center for Type Culture Collection (CCTCC). Both cells were cultured in DMEM (Gibco BRL, Grand Island, NY, USA) containing 10% fetal bovine serum (FBS), 1% penicillin/streptomycin (Gibco BRL, Grand Island, NY, USA) at 37 °C and 5% CO_2. The medium was replaced every three days, and 0.25% trypsin in PBS was used for cell passage. Each well of the 6-well plate was seeded with 2×10^5 cells and cultured for 24 h. Cells were respectively transfected with mimics, inhibitor of mmu-miR-92a-2-5p or the nonspecific (NC)-mimics at a final concentration of 50 nmol/L using ribo*EFCT*™ CP (RIBBIO, Guangzhou) following the manufacturer's instructions. The cells were harvested 48 h after transfection.

2.6. RNA isolation, reverse transcription (RT) and real-time PCR analysis

Total RNAs from cell lysates and liver tissue were isolated using TRIzol reagent (Life Technologies, Carlsbad, CA) following the instructions given by the manufacturer. MiRNA was extracted using a mirVana miRNA isolation kit (Ambion, Carlsbad, CA, USA). RNA was assessed for quantity and quality using a NanoDrop ND1000 (Thermo Scientific, Wilmington, DE, USA). Mmu-miR-92a-2-5p was reverse transcribed using a specific stem-loop primer (Applied Biosystems, Carlsbad, CA, USA). The cDNAs were synthesized using the PrimeScript RT Master Mix (Takara, Dalian, China), and quantitative PCRs were performed using SYBR Premix Ex Taq II (Takara, Dalian, China). LightCycler® 480 System (Hoffmann-La Roche Ltd., Basel, Switzerland) was used for observing the relative expression of mRNA and miRNA. Using the $2^{-\Delta\Delta Ct}$ method the relative expression of cytokines, miR-29b-

Table 1
The primers of qRT-PCR.

Gene		Primers (5′-3′)
Mmu-Tlr2	Forward	CTGATGGAGGTGGAGTTTGA
	Reverse	TCCGTATTGTTACCGTTTCTA
Mmu-miR-92a-2-5p	Forward	ATCGTACGTGGGAGGTGGGGA
	Reverse	GCAGGGTCCGAGGTATTC
Mmu-α-SMA	Forward	TCCCTGGAGAAGAGCTACGAA
	Reverse	ATAGGTGGTTTCGTGGATGCC
Mmu-Colla I	Forward	TGACTGGAAGAGCGGAGAGT
	Reverse	AGACGGCTGAGTAGGGAACA
Mmu-GAPDH	Forward	GGTTGTCTCCTGCGACTTCA
	Reverse	TGGTCCAGGGTTTCTTACTCC
U6	Forward	GCTTCGGCAGCACATATA CTAAAAT
	Reverse	CGCTTCACGAATTTGCGTG TCAT
IFN-γ	Forward	AGCAACAACATAAGCGTCAT
	Reverse	CCTCAAACTTGGCAATACTC
IL-4	Forward	CATCCTGCTCTTCTTTCTCG
	Reverse	CCTTCTCCTGTGACCTCGTT
TNF-α	Forward	TTGACCTCAGCGCTGAGTTG
	Reverse	CCTGTAGCCCACGTCGTAGC

3p and the targeted genes against U6 or GAPDH was calculated. Primers sequences are given in Table 1.

2.7. ELISA

The cytokine assays for IFN-γ, TNF-α and IL-4 in sera of mice were determined by using mouse cytokine assay kits (Ebioscience, San Diego, USA) according to the manufacturer's instructions.

2.8. Western-blotting

Total proteins from liver tissues or cells were extracted using RIPA lysis buffer (Beyotime, China). The protein concentration of samples was quantified by BCA Protein Assay Kit (Cwbiotech, Beijing, China). 30 μg protein sample ran in 10% sodium dodecyl sulfate-polyacrylamide gel electrophoresis (SDS-PAGE), and then transferred to polyvinylidene difluoride membranes (PVDF, 100 V, 40 min) using electrotransfer method. The membranes were subsequently blocked with 10% skim milk in TBST for 2 h to block non-specific binding, and then probed with primary antibodies against *TLR2* (Rabbit polyclonal, ab191458, 1:500, Abcam, Cambridge, MA, USA), α-SMA (Rabbit polyclonal, ab191458, 1:1000, Abcam), Collagen I (Rabbit polyclonal, ab138492, 1:500, Abcam) and GAPDH (Rabbit monoclonal, ab181603, 1:10000, Abcam) incubated at 4 °C overnight. The membranes were washed 3 times with 0.2% tween-PBS (TBST), and then were probed with secondary antibody and incubated at 37 °C for an hour. Finally, after being washed 3 times with TBST, the membranes were visualized with ECL-chemiluminescence kit. GAPDH was used as an internal control to verify basal level expression and equal protein loading.

2.9. Dual-luciferase reporter assay

The wild-type and mutated 3'-UTR of *TLR2* were cloned into multiple cloning sites of pGL3 vectors (Promega, Madison, WI, USA). The recombinant plasmids were co-transfected with mimics, inhibitor of mmu-miR-92a-2-5p or the nonspecific (NC)-mimics via Lipofectamine 2000 (Invitrogen, Carlsbad, CA, USA) in 293T cells. Dual luciferase reporter assay system obtaining from Promega (Madison, WI, USA) was performed to evaluate the firefly and renilla luciferase activities. The relative luciferase activity in each group was presented in the ratio of firefly luciferase activity to renilla luciferase activity.

2.10. CCK-8 assay

Cell viability was determined using CCK-8 assay. Briefly, NIH/3T3 were plated at a density of 1×10^4 cells per well in 96-well plates. After transfected with mimics, inhibitor of mmu-miR-92a-2-5p or the non-specific (NC)-mimics 48 h, 10 μL of CCK-8 solution (Beyotime, Shanghai, China) was added to each well for 4 h at 37 °C in a 5% CO_2 incubator. The absorbance was determined at 450 nm using a SpectraMax i3x Multi-Mode Detection Platform (Molecular Devices, USA).

2.11. Flow cytometry

NIH-3T3 fibroblasts were randomly divided into four groups, and respectively transfected with mmu-miR-92a-2-5p NC, mimic and inhibitor. The apoptosis ratio of four group cells was determined via FCM assay using Annexin V/PI detection kit (KeyGene, Nanjing, China) and Bd Biosciences (Mansfield, mA, USA). About 5×10^5 cells/mL were added into 6-well plates and cultured for 48 h. Before pre-cold ethanol being performed to fix the cells, single cell suspensions were collected. Afterwards, cells were incubated with propidium iodide (PI) as well as Annexin V to analyze apoptosis ratio.

2.12. Statistical analysis

All quantitative values were presented as the mean ± standard deviation (S.D.). Unpaired student's *t*-test was utilized to obtain differences between groups. And the differences among the groups of samples were accomplished by One-way ANOVA. All of the statistical analyses were made using GraphPad Prism v6.0 (GraphPad Software, Inc.). A value of $P < 0.05$ was considered statistically significant.

3. Results

3.1. TLR2 was up-regulated in the progression of S. japonicum-induced liver fibrosis

Based on microarray platform GPL6105 as well as microarray data GSE14367, differentially expressed genes and dysregulated pathways were determined via R language and KEGG database. Total 156 differentially expressed genes were identified in liver tissue at 7 weeks after *S. japonicum* infection compared with uninfected groups (Fig. 1A, B). Toll-like receptor signaling pathway was up-regulated in liver tissue at 7 weeks after *S. japonicum* infection compared with uninfected groups (Fig. 1C, D). Further, we analyzed the overlap of dysregulated gene between gene sets at 7 weeks after *S. japonicum* infection and genes in Toll-like receptor signaling pathway. We found 2 up-regulated genes, including *TLR2* and Ctsk, and *TLR2* was chosen to further study (Fig. 1E). Liver tissues were harvested at 0, 2, 4, 6, 8, 10 weeks after *S. japonicum* infection. The qPCR results showed that the *TLR2* was significantly raised at 6, 8, 10 weeks after *S. japonicum* infection (Fig. 1F).

3.2. Mmu-miR-92a-2-5p was down-regulated in the progression of S. japonicum-induced liver fibrosis

Based on microarray platform GPL16016 and microarray data GSE63135, R language was utilized for analyzing the differentially expressed genes (Fig. 2A). Further, we analyzed the overlap of dysregulated miRNA in *S. japonicum* infection compared with un-infection groups and miRNA targeting *TLR2*. We found 1 up-regulated and 1 down-regulated miRNA in *S. japonicum* infection (Fig. 2B). Mmu-miR-92a-2-5p was down-regulated at 4, 6, 8 or 10 weeks after *S. japonicum* infection compared with 0 week (Fig. 2C). Bioinformatics analysis predicted that *TLR2* 3' UTR was a potential target of mmu-miR-92a-2-5p (Fig. 2D). Wild-type and the mutated sequences of *TLR2* 3' UTR, together with the complimentary mmu-miR-92a-2-5p sequence, were shown (Fig. 2D). These bioinformatic analyses indicated that mmu-miR-92a-2-5p might directly target 3' UTR of *TLR2*.

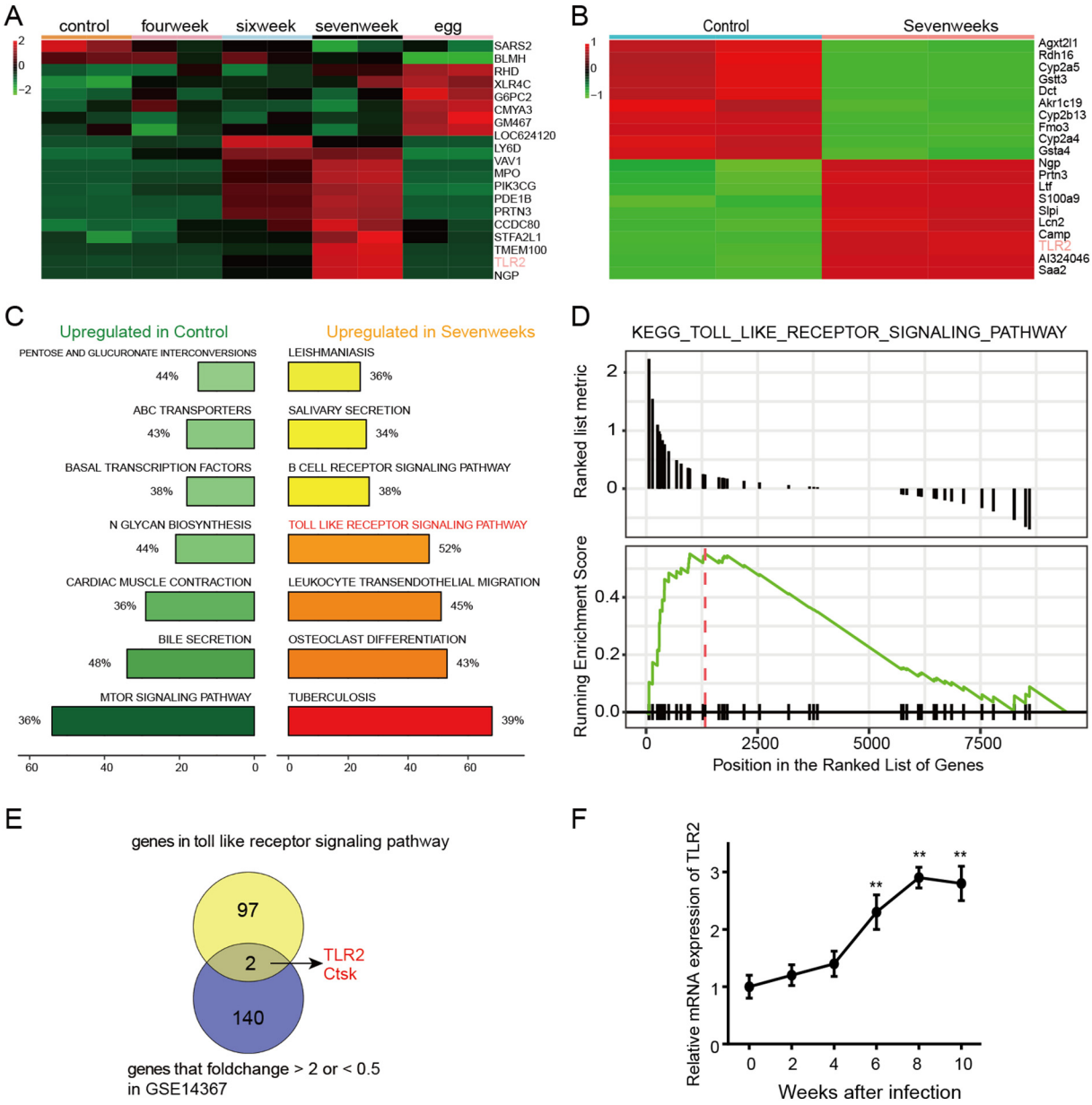

Fig. 1. *TLR2* expressions were upregulated in *S. japonicum* infected mice. (A, B) Heatmap showing top differentially expressed genes in different weeks after *S. japonicum* infection compared with control group. (C) Seven most up-regulated KEGG pathways in control and seven weeks groups respectively ranked by the normalized enrichment score (NES). (D) GSEA enrichment plots of genes involved in the TOLL_LIKE_RECEPTOR_SIGNALING_PATHWAY in control and with *S. japonicum* infection 7 weeks. Most genes involved in this pathway were up-regulated as the ranked list metric and running enrichment score were < 0. (E) Venn diagram showing the overlap of dysregulated gene between gene sets at 7 weeks after *S. japonicum* infection and genes in TOLL_LIKE_RECEPTOR_SIGNALING_PATHWAY. (F) The mRNA expressions of *TLR2* at 0, 2, 4, 6, 8 or 10 weeks after infection by qRT-PCR. The expression fold in *S. japonicum* infected groups was calculated compared with the uninfected groups; all data are mean ± SD, $n = 4$, $^{*}p < 0.05$, $^{**}p < 0.01$.

3.3. Lentivirus-mediated over-expression of mmu-miR-92a-2-5p relieves S. japonicum-induced liver pathological damage

Lenti-mmu-miR-92a-2-5p or Lenti-NC was intravenously injected into *S. japonicum*-infected mice via the tail vein on day 10 post-infection, respectively. As demonstrated by qRT-PCR, hepatic mmu-miR-92a-2-5p expression considerably increased in *S. japonicum*-infected mice injected with lenti-mmu-miR-92a-2-5p (Fig. 3A). Hepatic *TLR2* mRNA expression obviously increased in *S. japonicum*-infected mice compared with un-infected mice while *TLR2* mRNA expression markedly reduced in *S. japonicum*-infected mice injected with lenti-mmu-miR-92a-2-5p compared with Lenti-NC or control group (Fig. 3B). Furthermore, the expressions of fibrotic genes, such as *α-SMA* and *colla I*, were significantly down-regulated in the *S. japonicum*-infected mice injected with Lenti-mmu-miR-92a-2-5p, as indicated by qRT-PCR (Fig. 3C, D). These data showed that mmu-miR-92a-2-5p inhibited *α-SMA* and *colla I* expressions in vivo, which indicated that mmu-miR-92a-2-5p can suppress liver fibrosis induced by *S. japonicum*. To investigate the hepatopathology in the *S. japonicum*-infected mice, the fixed livers were stained with HE or Masson's trichrome (Fig. 3E, F). H&E staining showed that the deposition of *S. japonicum* egg granulomas in the livers from *S. japonicum*-infected mice injected with Lenti-mmu-miR-92a-2-5 were significantly decreased in comparison with Lenti-NC group (Fig. 3G). Fibrotic collagen deposition around the egg granulomas was stained with blue color by Masson's trichome staining. Consistently, the formation of collagenous fiber was greatly declined in

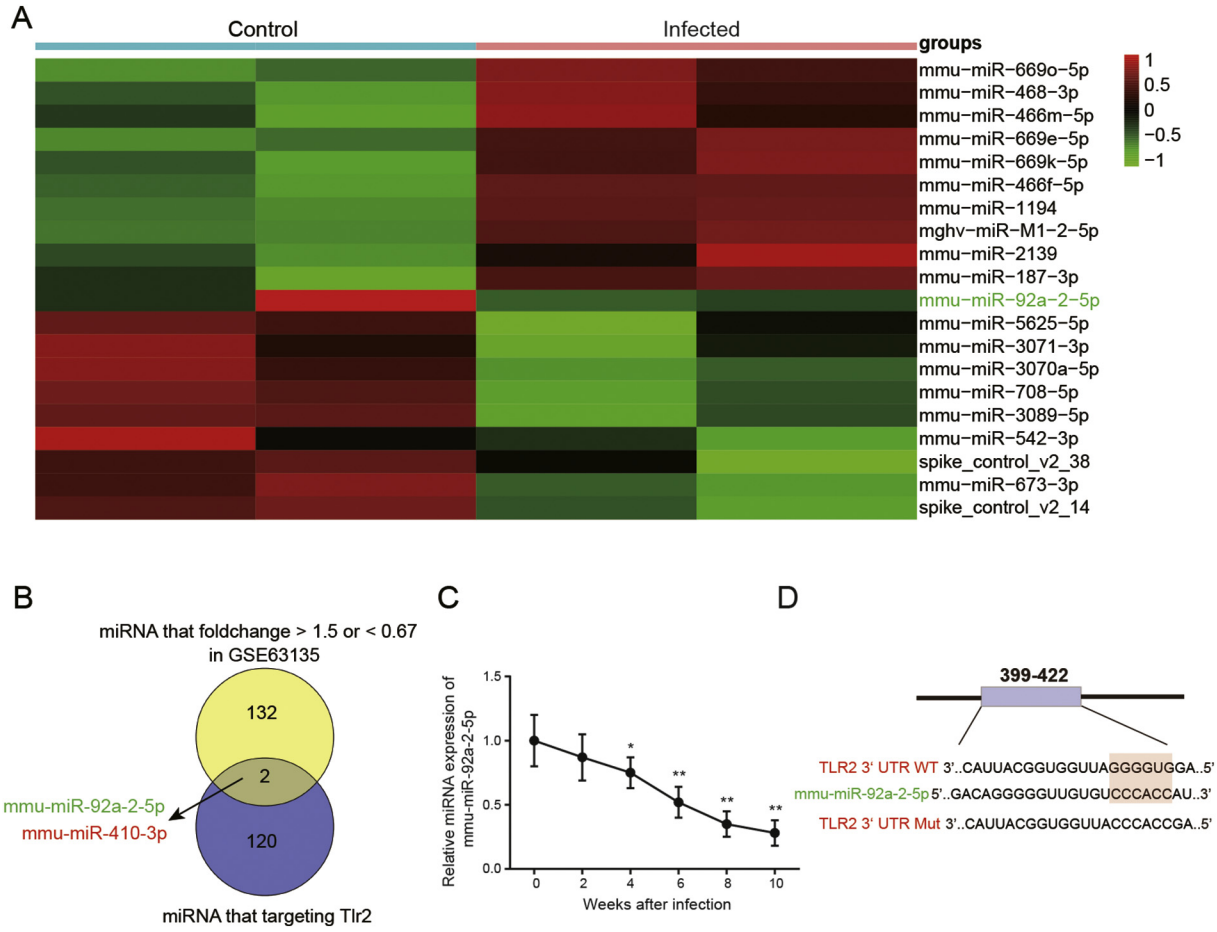

Fig. 2. mmu-miR-92a-2-5p targeted 3' UTR of *TLR2*. (A) Heatmap showing differentially expressed genes between control and *S. japonicum* infection in microarray data GSE63135. (B) Venn diagram showing the overlap of dysregulated miRNA after *S. japonicum* infection (foldchange $>$ 1.5 or $<$ 0.67) and miRNA which could target *TLR2*. (C) The expressions of mmu-miR-92a-2-5p at 0, 2, 4, 6, 8 or 10 weeks after infection by qRT-PCR. The expression fold in *S. japonicum* infected groups were calculated compared with the uninfected groups; $n = 5$, $^{*}p < 0.05$, $^{**}p < 0.01$, compared with 0 week. (D) Bioinformatics analysis predicted that *TLR2* 3' UTR was a potential target of mmu-miR-92a-2-5p.

Lenti-mmu-miR-92a-2-5 group (Fig. 3H). These observations suggested that mmu-miR-92a-2-5p overexpression could ameliorate liver fibrosis in vivo.

3.4. Mmu-miR-92a-2-5p inhibited NIH-3 T3 cells vitality and suppressed fibrosis of its fibroblasts

The relative expression of mmu-miR-92a-2-5p in NIH-3 T3 fibroblasts was significantly higher in the mmu-miR-92a-2-5p mimic group than that in the NC group (Fig. 4A). Cells transfected with mmu-miR-92a-2-5p inhibitor significantly inhibited mmu-miR-92a-2-5p expression (Fig. 4A). CCK-8 assays revealed that mmu-miR-92a-2-5p mimic transfection significantly inhibited NIH-3 T3 fibroblasts viability while mmu-miR-92a-2-5p inhibitor transfection enhanced NIH-3 T3 fibroblasts viability (Fig. 4B). The NIH-3 T3 fibroblasts in the mmu-miR-92a-2-5p mimic groups showed higher cell apoptosis ratio, while the apoptosis ratio of cells in mmu-miR-92a-2-5p inhibitor groups was lower compared with control and NC groups (Fig. 4C, D). Consistently, the expression levels of typical indicators for fibrosis, *Colla I* and *α-SMA*, were significantly elevated in mmu-miR-92a-2-5p inhibitor groups while mmu-miR-92a-2-5p mimic inhibited the mRNA expression of *Colla I* and *α-SMA* (Fig. 4E, F). Moreover, at the protein level, potent inhibition of *Colla I* and *α-SMA* by mmu-miR-92a-2-5p mimic was confirmed by western blot in NIH/3T3 cells (Fig. 4G).

3.5. mmu-miR-92a-2-5p suppressed TRL2 protein expression and related cytokines in S. japonicum-induced liver fibrosis

To validate the analysis of microarray data GSE63135 in which *TLR2* was the target of mmu-miR-92a-2-5p, we examined the levels of *TLR2* in vitro and in vivo. In NIH/3T3 cells, western blot showed that mmu-miR-92a-2-5p mimic group obviously inhibited *TLR2* protein expression while mmu-miR-92a-2-5p inhibitor group increased *TLR2* protein expression (Fig. 5A). Luciferase report assay showed that mmu-miR-92a-2-5p mimic reduced luciferase activities and mmu-miR-92a-2-5p inhibitor increased luciferase activities compared with NC and control groups (Fig. 5B). Further, in *S. japonicum*-infected mice, western blot results suggested that *TLR2* protein was markedly upregulated in liver tissues 10 weeks after *S. japonicum* infection compared with 0 week (Fig. 5C). It has been reported that TLR1/TLR2 could activate NF-κB signaling pathways and various pro-inflammatory cytokines. Thus, we detected related cytokines by ELISA. Serum IL-4, IFN-γ and TNF-α expression levels were decreased in Lenti-mmu-miR-92a-2-5p group when compared with the groups of Lenti-NC or control groups (Fig. 5D–F). In addition, qRT-PCR results showed that mRNA levels of IL-4, IFN-γ and TNF-α reduced in the fibrotic livers of Lenti-mmu-miR-92a-2-5p group (Fig. 5G–I), which is consistent with ELISA data. These results demonstrated that mmu-miR-92a-2-5p could directly target *TLR2*.

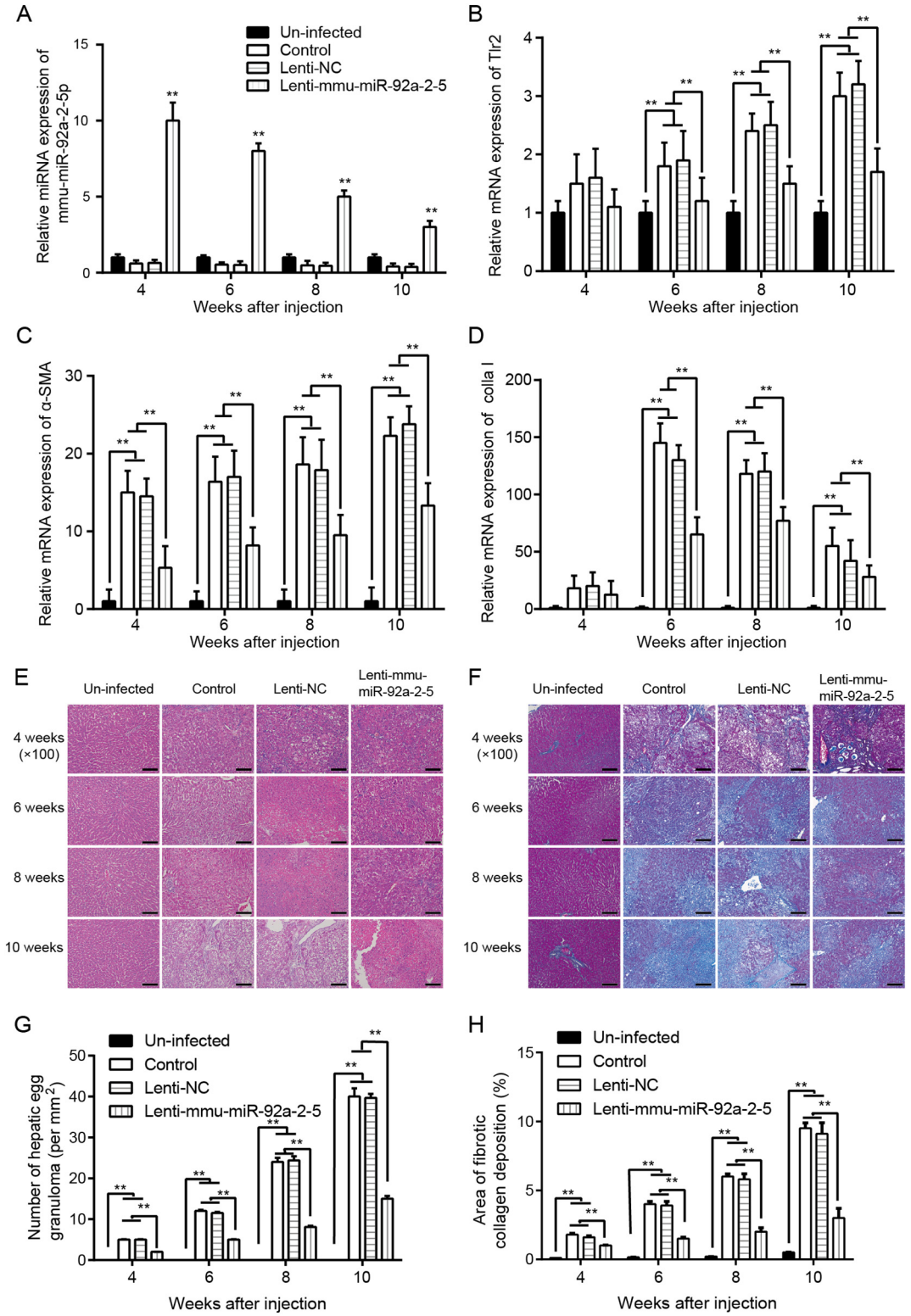

Fig. 3. Mmu-miR-92a-2-5p in *S. japonicum*-infected mice liver pathological damage. (A) The relative expression of mmu-miR-92a-2-5p at 4, 6, 8 or 10 weeks after infection was detected by qRT-PCR. (B) The relative mRNA expression of *TLR2* at 4, 6, 8 or 10 weeks after infection was detected by qRT-PCR. (C–D) *α-SMA* and *Colla I* mRNA expression at 4, 6, 8 or 10 weeks were detected by qRT-PCR. The expression folds in the infected groups were calculated with un-infected groups. $^{**}p < 0.01$. Representative images of liver tissues in different groups stained with HE (◊100) (E) and Masson's trichome (◊100) (F). (G) The number of hepatic egg granulomas in different groups at 4, 6, 8 or 10 weeks after infection was calculated and expressed as per area of the liver ($mm^{2)}$. (H) Hepatic collagen deposition was quantified using Image-Pro Plus 6.0. $^{**}p < 0.01$. Scale bar = 50 μm.

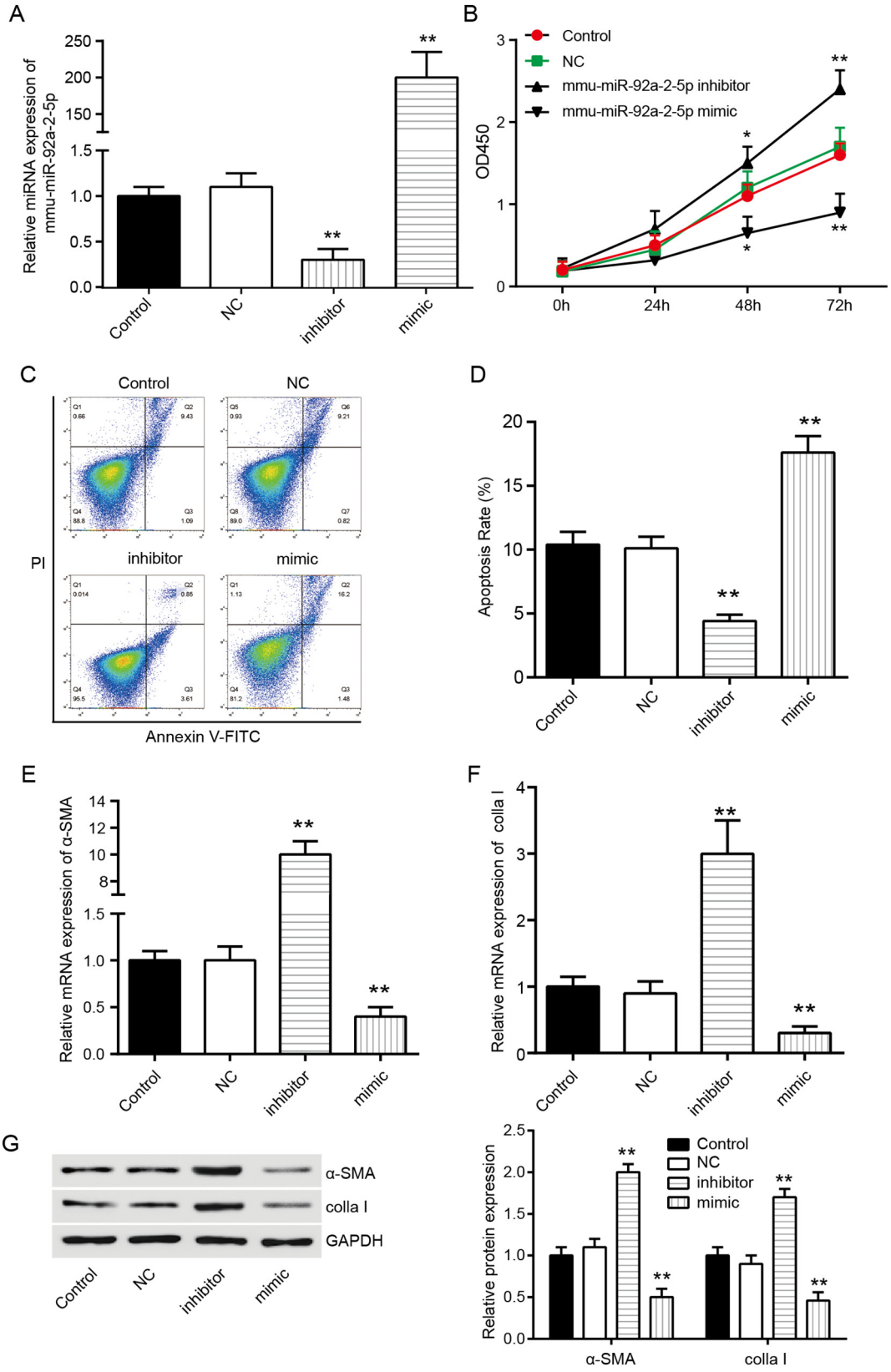

Fig. 4. Downregulation of mmu-miR-92a-2-5p reduced NIH-3 T3 cells vitality and promoted fibrosis of NIH-3 T3 fibroblasts. (A) The relative expression of mmu-miR-92a-2-5p was shown in NIH-3T3 fibroblasts. $^{**}p < 0.01$ vs control or mmu-miR-92a-2-5p NC. (B) The OD value of NIH-3T3 fibroblasts at 450 nm in the four groups detected by CCK-8 assay. $^{*}p < 0.05$, $^{**}p < 0.01$ vs. control or mmu-miR-92a-2-5p NC. (C&D) Flow cytometry showed apoptosis ratio of NIH/3T3 cells after transfected with mmu-miR-92a-2-5p NC, mimic and inhibitor. (E&F) *α-SMA* and *colla I* mRNA expression was detected by qRT-PCR in NIH-3T3 fibroblasts in the four groups. $^{**}p < 0.01$ vs control or mmu-miR-92a-2-5p NC. (G) Western blot assay detected the *α-SMA* and *collaI* expression in NIH-3T3 fibroblasts in the four groups. $^{**}p < 0.01$ vs control or mmu-miR-92a-2-5p NC.

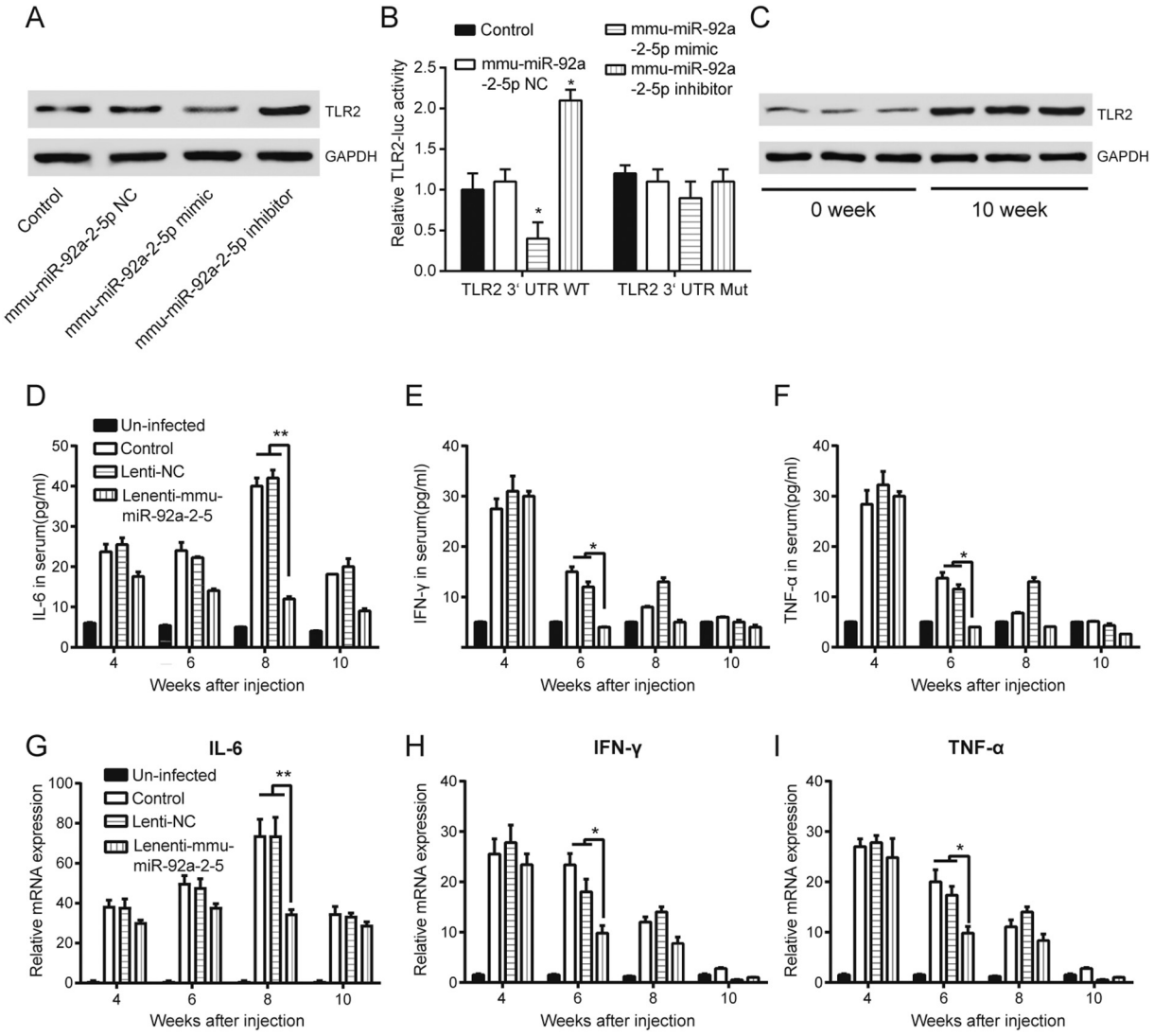

Fig. 5. mmu-miR-92a-2-5p regulated the expression of *TRL2* and related cytokines
(A) The western blot showed the protein expressions of *TLR2* in NIH-3T3 fibroblasts in the four groups. (B) Luciferase report assay of TLR2-luc treated with mmu-miR-92a-2-5p mimic, mmu-miR-92a-2-5p inhibitor or mmu-miR-92a-2-5p NC, $*p < 0.05$ vs. control or mmu-miR-92a-2-5p NC. (C) The western blot showed the protein expressions of *TLR2* at 0 and 10 weeks after infection in vivo. (D-F) The ELISA revealed the levels of cytokines IL-4, IFN-γ and TNF-α in serum. (G-I) The mRNA expression of cytokines was determined by qRT-PCR. $*p < 0.05$, $**p < 0.01$ vs control or mmu-miR-92a-2-5p NC.

3.6. S. japonicum-induced liver pathological damage could be relieved in TLR2 knockout mice

To further explore the relation between mmu-miR-92a-2-5p and *TLR2* and the role of *TLR2* in *S. japonicum*-induced liver fibrosis, *TLR2* knockout mice was established. Similarly, Lenti-mmu-miR-92a-2-5p was percutaneously injected into *S. japonicum*-infected $TLR2^{-/-}$ mice via percutaneously injection (Lenti-mmu-miR-92a-2-5 Tlr2 KO group). As shown in Fig. 6A and B, the expressions of fibrotic genes *α-SMA* and *colla I* were significantly down-regulated in the $TLR2^{-/-}$ mice injected with or without Lenti-mmu-miR-92a-2-5p by qRT-PCR. The knockout of *TLR2* reduced more *α-SMA* and *colla I* than normal mice injected with Lenti-mmu-miR-92a-2-5p, which further implied that *TLR2* was the target of the mmu-miR-92a-2-5p. H&E and Masson's trichome staining showed that the deposition of *S. japonicum* egg granulomas and fibrotic collagen deposition in the livers were significantly decreased in in the $TLR2^{-/-}$ mice injected with or without Lenti-mmu-miR-92a-2-5p (Fig. 6C–F).

4. Discussion

In the present study, mmu-miR-92a-2-5p and *TLR2* expression levels were investigated in the mice with *S. japonicum* infection, then their dysregulation was found in injected mice compared with normal mice. Besides, *TLR2* knockout mice were established to further investigate their relations. Otherwise, in our study, mmu-miR-92a-2-5p was found to play a suppressive role in the progression of liver fibrosis via regulating *TLR2*.

According to previous investigation, *S. japonicum* infection usually caused granulomatous inflammation in that deposition of parasite eggs, resulting in dysregulation of immune system, activation of hepatic stellate cells and even continuously liver fibrosis [21]. To evaluate the specific molecular mechanism of *S. japonicum* induced liver fibrosis, some related pathways and deregulating genes were predicted by bioinformatics analysis, and further study showed that the over-expression of *TLR2* and low-expression of mmu-miR-92a-2-5p were discovered by qRT-PCR and western blot analysis. Similarly, Lin et al. demonstrated that *TLR2* and *TLR4* were up-regulated in obstructive jaundice-induced liver fibrosis and inhibiting their expressions could

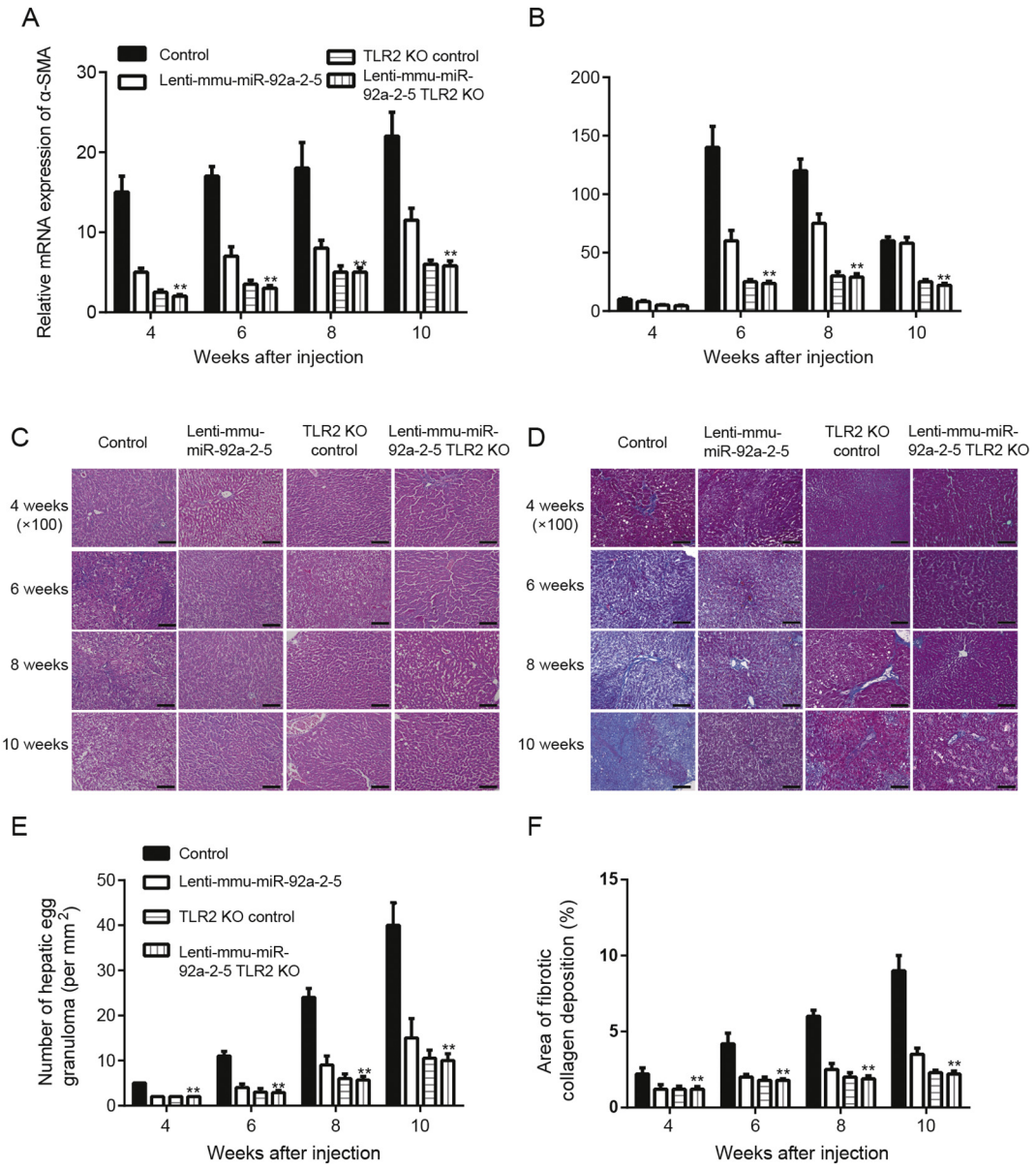

Fig. 6. TLR2$^{-/-}$ ameliorated *S. japonicum*-induced liver fibrosis
(A&B) *α-SMA* and *Colla I* mRNA expression at 4, 6, 8 or 10 weeks were detected by qRT-PCR. (A&B) Liver tissues in four groups stained with HE (×100) (C) and Masson's trichome (×100) (D). Scale bar = 50 μm. (E) The number of hepatic egg granulomas at 4, 6, 8 or 10 weeks after infection was measured as per area of the liver (mm^2). (F) Hepatic collagen deposition was quantified using Image-Pro Plus 6.0. $^{**}p < 0.01$ vs control group.

relieve the situation [22]. Furthermore, *TLR2* played a crucial role in acute and chronic liver injury induced by CCl_4 injecting in the mouse [23]. Besides, as demonstrated by previous researches, liver cirrhosis and the secondary affection might be regulated and controlled by *TLR2* [24]. All in all, these research results indicated that dysregulation of *TLR2* was closely correlated with liver fibrosis induced by *S. japonicum*.

However, how mmu-miR-92a-2-5p was involved in pathological process and whether it regulated *TLR2* expression in liver fibrosis were fairly blurring. Moreover, miRNAs down-regulating target gene expression by binding 3'UTR region had been uncovered [25]. Therefore, dual-luciferase reporter gene assay was utilized to determine if mmu-miR-92a-2-5p targeted *TLR2* expression, with the results that mmu-miR-92a-2-5p could bind with *TLR2* promoter region and repress its expression. As primary sensors of microbial products, TLRs are pattern recognition receptors which play a critical role in the response against distinct, structurally conserved components of pathogens [7]. It has been reported that *TLR2* agonist was associated with an increase in IFN-γ, IL-12, IL-10 and other cytokines [26]. Thus we determined cytokines IL-4, IFN-γ and TNF-α in Lenti-mmu-miR-92a-2-5p group as the evidence of mmu-miR-92a-2-5p in regulation of *TLR2*. Moreover, the *TLR2* knockout mice models were also constructed to further confirm this hypothesis. In the study of Ye et al., miRNA-145 could contribute to liver fibrosis via targeting adducin 3 in biliary atresia [19]. Besides, the expression of *Colla I* and *α-SMA* which were two major hepatic stellate cell activation related proteins would be hindered by miRNA-338-3p via targeting CDK4 [16]. Furthermore, Ma et al. reported that miR-200c might influence liver fibrosis via targeting FOG2/PI3K signal pathway [27]. Analogous results, that mmu-miR-92a-2-5p transfection would inhibit the expression of typical indicators for fibrosis, *Colla I* and *α-SMA*, had been gotten in our study.

In the last decade, genetic studies demonstrated that miR-92a played a critical role in cancer pathogenesis as well as normal development [28]. For example, Li et al. reported that miR-92a regulated cell proliferation via targeting TGFB pathway to influence normal

development of palatal mesenchyme [29]. Besides, in seischemia-reperfusion mouse, that miR-92a could promote cell apoptosis, was illustrated by Jiang et al. [30]. But, the research focused on the effects of mmu-miR-92a-2-5p on liver fibrosis was poor. In our research, the animal and cell models were transfected with mmu-miR-92a-2-5p, finding that mmu-miR-92a-2-5p down-regulating the expression of *TLR2* to relieve the liver fibrosis induced by *S. japonicum*.

While our study tried to give consideration to all aspects, some inadequacies still existed. For example, in the present study, mmu-miR-92a-2-5p injection would suppress the expression of *Colla I* and *α-SMA*, but the underlying molecular mechanism wasn't investigated.

In conclusion, our investigation demonstrated that mmu-miR-92a-2-5p could attenuate the expression of liver fibrosis-related proteins and regulate cell viability to prevent *Schistosoma japonicum*-induced liver fibrosis by targeting *TLR2*. In according to above study, mmu-miR-92a-2-5p might become a promising treatment strategy for *S. japonicum*-induced liver fibrosis.

Funding

The study was supported by Guangxi Nature Fund Project, Gui Keji [2016] 380, Experimental Study on the Treatment of Mice with Secondary Alveolar Echinococcosis by MAPK Signal Pathway Inhibitor Based on Full-Length cDNA Library.

Declaration of conflict of interest

The authors declare that they have no conflict of interest.

Ethics approval

All animal experiments were consent with the animal ethics standard of the Second Affiliated Hospital of Guilin Medical University.

Informed consent

Not applicable.

References

[1] D.G. Colley, A.L. Bustinduy, W.E. Secor, C.H. King, Human schistosomiasis, Lancet 383 (2014) 2253–2264.
[2] T. Vos, A.D. Flaxman, M. Naghavi, R. Lozano, C. Michaud, M. Ezzati, et al., Years lived with disability (YLDs) for 1160 sequelae of 289 diseases and injuries 1990–2010: a systematic analysis for the Global Burden of Disease Study 2010, Lancet 380 (2012) 2163–2196.
[3] J. Tang, H. Huang, X. Ji, X. Zhu, Y. Li, M. She, et al., Involvement of IL-13 and tissue transglutaminase in liver granuloma and fibrosis after schistosoma japonicum infection, Mediat. Inflamm. 2014 (2014) 753483.
[4] A.G. Ross, R.M. Olveda, L. Acosta, D.A. Harn, D. Chy, Y. Li, et al., Road to the elimination of schistosomiasis from Asia: the journey is far from over, Microbes Infect. 15 (2013) 858–865.
[5] W. Wu, A. Feng, Y. Huang, Research and control of advanced schistosomiasis japonica in China, Parasitol. Res. 114 (2015) 17–27.
[6] J.Y. Kang, J.O. Lee, Structural biology of the toll-like receptor family, Annu. Rev. Biochem. 80 (2011) 917–941.
[7] J.B. Soares, P. Pimentel-Nunes, L. Afonso, C. Rolanda, P. Lopes, R. Roncon-Albuquerque Jr.et al., Increased hepatic expression of TLR2 and TLR4 in the hepatic inflammation-fibrosis-carcinoma sequence, Innate Immun. 18 (2012) 700–708.
[8] K. Machida, H. Tsukamoto, H. Mkrtchyan, L. Duan, A. Dynnyk, H.M. Liu, et al., Toll-like receptor 4 mediates synergism between alcohol and HCV in hepatic oncogenesis involving stem cell marker Nanog, Proc. Natl. Acad. Sci. U. S. A. 106 (2009) 1548–1553.
[9] L. Ji, R. Xue, W. Tang, W. Wu, T. Hu, X. Liu, et al., Toll like receptor 2 knock-out attenuates carbon tetrachloride (CCl4)-induced liver fibrosis by downregulating MAPK and NF-kappaB signaling pathways, FEBS Lett. 588 (2014) 2095–2100.
[10] Y. Gao, L. Chen, M. Hou, Y. Chen, M. Ji, H. Wu, et al., TLR2 directing PD-L2 expression inhibit T cells response in *Schistosoma japonicum* infection, PLoS One 8 (2013) e82480.
[11] Q. Liu, G. Wang, Y. Chen, G. Li, D. Yang, J. Kang, A miR-590/Acvr2a/Rad51b axis regulates DNA damage repair during mESC proliferation, Stem Cell Rep. 3 (2014) 1103–1117.
[12] C. Seeliger, E.R. Balmayor, M. van Griensven, miRNAs related to skeletal diseases, Stem Cells Dev. 25 (2016) 1261–1281.
[13] F. Marra, Hepatic stellate cells and the regulation of liver inflammation, J. Hepatol. 31 (1999) 1120–1130.
[14] Y. Sekiya, T. Ogawa, K. Yoshizato, K. Ikeda, N. Kawada, Suppression of hepatic stellate cell activation by microRNA-29b, Biochem. Biophys. Res. Commun. 412 (2011) 74–79.
[15] F. Yu, Y. Guo, B. Chen, P. Dong, J. Zheng, MicroRNA-17-5p activates hepatic stellate cells through targeting of Smad7, Lab. Investig. 95 (2015) 781–789.
[16] B. Duan, J. Hu, T. Zhang, X. Luo, Y. Zhou, S. Liu, et al., miRNA-338-3p/CDK4 signaling pathway suppressed hepatic stellate cell activation and proliferation, BMC Gastroenterol. 17 (2017) 12.
[17] C. Roderburg, G.W. Urban, K. Bettermann, M. Vucur, H. Zimmermann, S. Schmidt, et al., Micro-RNA profiling reveals a role for miR-29 in human and murine liver fibrosis, Hepatology 53 (2011) 209–218.
[18] K. Wu, C. Ye, L. Lin, Y. Chu, M. Ji, W. Dai, et al., Inhibiting miR-21 attenuates experimental hepatic fibrosis by suppressing both the ERK1 pathway in HSC and hepatocyte EMT, Clin. Sci. 130 (2016) 1469–1480.
[19] Y. Ye, Z. Li, Q. Feng, Z. Chen, Z. Wu, J. Wang, et al., Downregulation of microRNA-145 may contribute to liver fibrosis in biliary atresia by targeting ADD3, PLoS One 12 (2017) e0180896.
[20] Y. Hayashita, H. Osada, Y. Tatematsu, H. Yamada, K. Yanagisawa, S. Tomida, et al., A polycistronic microRNA cluster, miR-17-92, is overexpressed in human lung cancers and enhances cell proliferation, Cancer Res. 65 (2005) 9628–9632.
[21] J. Luo, Y. Liang, F. Kong, J. Qiu, X. Liu, A. Chen, et al., Vascular endothelial growth factor promotes the activation of hepatic stellate cells in chronic schistosomiasis, Immunol. Cell Biol. 95 (2017) 399–407.
[22] Y.C. Lin, F.S. Wang, Y.L. Yang, Y.T. Chuang, Y.H. Huang, MicroRNA-29a mitigation of toll-like receptor 2 and 4 signaling and alleviation of obstructive jaundice-induced fibrosis in mice, Biochem. Biophys. Res. Commun. 496 (2018) 880–886.
[23] A. Moles, L. Murphy, C.L. Wilson, J.B. Chakraborty, C. Fox, E.J. Park, et al., A TLR2/S100A9/CXCL-2 signaling network is necessary for neutrophil recruitment in acute and chronic liver injury in the mouse, J. Hepatol. 60 (2014) 782–791.
[24] H.D. Nischalke, C. Berger, K. Aldenhoff, L. Thyssen, M. Gentemann, F. Grunhage, et al., Toll-like receptor (TLR) 2 promoter and intron 2 polymorphisms are associated with increased risk for spontaneous bacterial peritonitis in liver cirrhosis, J. Hepatol. 55 (2011) 1010–1016.
[25] T. Duellman, C. Warren, J. Yang, Single nucleotide polymorphism-specific regulation of matrix metalloproteinase-9 by multiple miRNAs targeting the coding exon, Nucleic Acids Res. 42 (2014) 5518–5531.
[26] M. Patel, D. Xu, P. Kewin, B. Choo-Kang, C. McSharry, N.C. Thomson, et al., TLR2 agonist ameliorates established allergic airway inflammation by promoting Th1 response and not via regulatory T cells, J. Immunol. 174 (2005) 7558–7563.
[27] T. Ma, X. Cai, Z. Wang, L. Huang, C. Wang, S. Jiang, et al., miR-200c accelerates hepatic stellate cell-induced liver fibrosis via targeting the FOG2/PI3K pathway, Biomed. Res. Int. 2017 (2017) 2670658.
[28] J.T. Mendell, miRiad roles for the miR-17-92 cluster in development and disease, Cell 133 (2008) 217–222.
[29] L. Li, J.Y. Shi, G.Q. Zhu, B. Shi, MiR-17-92 cluster regulates cell proliferation and collagen synthesis by targeting TGFB pathway in mouse palatal mesenchymal cells, J. Cell. Biochem. 113 (2012) 1235–1244.
[30] C. Jiang, N. Ji, G. Luo, S. Ni, J. Zong, Z. Chen, et al., The effects and mechanism of miR-92a and miR-126 on myocardial apoptosis in mouse ischemia-reperfusion model, Cell Biochem. Biophys. 70 (2014) 1901–1906.